

Human C5-specific single-chain variable fragment ameliorates brain injury in a model of NMOSD

Wenli Zhu, MD, Zhen Wang, MD, Suying Hu, PhD, Ye Gong, PhD, Yuanchu Liu, PhD, Huanhuan Song, PhD, Xiaoli Ding, PhD, Ying Fu, MD, and Yaping Yan, PhD

Correspondence

Dr. Yan
yaping.yan@snnu.edu.cn

Neurol Neuroimmunol Neuroinflamm 2019;6:e561. doi:10.1212/NXI.0000000000000561

Abstract

Objective

Using phage display, we sought to screen single-chain variable fragments (scFvs) against complement C5 to treat neuromyelitis optica spectrum disorder (NMOSD).

Methods

After 5 rounds of phage display, we isolated individual clones and identified phage clones specifically binding to C5 using ELISA. Using aquaporin-4 (AQP4)-transfected cells in vitro, we confirmed whether these scFvs prevented complement-dependent cytotoxicity (CDC) caused by the serum of patients with NMOSD and human complement (hC). We selected an NMOSD mouse model, in which intracerebral NMOSD immunoglobulin G (IgG) and hC injections induce NMOSD-like lesions in vivo.

Results

We obtained scFvs to test specificity and blocking efficiency. The scFv C5B3 neutralized C5 in the complement activation pathway, which prevented AQP4-IgG-mediated CDC in AQP4-transfected cells. In an NMOSD mouse model, C5B3 prevented AQP4 and astrocyte loss, decreased demyelination, and reduced inflammatory infiltration and membrane attack complex formation in lesions.

Conclusions

We used phage display to screen C5B3 against C5, which was effective in inhibiting cytotoxicity in vitro and preventing CNS pathology in vivo.

From the Key Laboratory of the Ministry of Education for Medicinal Resources and Natural Pharmaceutical Chemistry (W.Z., Z.W., S.H., Y.G., Y.L., H.S., X.D., Y.F., Y.Y.), National Engineering Laboratory for Resource Development of Endangered Crude Drugs in Northwest of China, College of Life Sciences, Shaanxi Normal University, Xi'an; Department of Neurology (W.Z.), Tianjin Neurological Institute, Tianjin Medical University General Hospital; and Department of Neurology (Z.W.), Xuanwu Hospital, Capital Medical University, Beijing, China.

Funding information and disclosures are provided at the end of the article. Full disclosure form information provided by the authors is available with the full text of this article at Neurology.org/NN.

The Article Processing Charge was funded by the authors.

This is an open access article distributed under the terms of the Creative Commons Attribution-NonCommercial-NoDerivatives License 4.0 (CC BY-NC-ND), which permits downloading and sharing the work provided it is properly cited. The work cannot be changed in any way or used commercially without permission from the journal.

Glossary

AQP = aquaporin-4; **BSA** = bovine serum albumin; **CDC** = complement-dependent cytotoxicity; **CHO** = Chinese hamster ovary; **GFAP** = glial fibrillary acidic protein; **hC** = human complement; **HAMA** = human anti-mouse antibody; **IBA** = ionized calcium-binding adaptor molecule; **IgG** = immunoglobulin G; **MAC** = membrane attack complex; **MBP** = myelin basic protein; **NMOSD** = neuromyelitis optica spectrum disorder; **PBS** = phosphate-buffered saline; **PFA** = paraformaldehyde; **SPR** = surface plasmon resonance.

Neuromyelitis optica spectrum disorder (NMOSD) is a disabling autoimmune disease of the CNS, which is characterized by optic neuritis and transverse myelitis.^{1,2} The discovery of autoantibodies against astrocytic aquaporin-4 immunoglobulin G (AQP4-IgG) distinguished NMOSD from MS based on its immunologic pathogenesis.^{3–5} Current NMOSD therapies, including general immunosuppressive agents, plasma exchange, and B-cell depletion, target AQP4-IgG and inflammatory reactions.^{6–8}

Complement plays a fundamental role in the pathogenesis of NMOSD.³ Complement can attack astrocytes through complement cascade activation and membrane attack complex (MAC; C5b-9) formation in astrocytic membranes.^{9,10} Moreover, secondary inflammatory cascades involving granulocytes and macrophage infiltration lead to demyelination and neuron death.^{11–14} Increasingly, NMOSD treatment studies have focused on complement C5. C5 can initiate the terminal complement cascade.¹⁵ Moreover, C5 inhibitor can prevent MAC formation by blocking complement-dependent cytotoxicity (CDC).¹⁶ Eculizumab, which is a therapeutic humanized monoclonal IgG that inhibits C5 convertase in the classical complement pathway, showed benefits in relapsing NMOSD.^{17–19}

Monoclonal antibody therapy is a new treatment strategy with high efficacy and tolerability in autoimmune diseases.^{6,20,21} However, most monoclonal antibodies are of a murine origin. The clinical application of murine monoclonal antibody-induced human anti-mouse antibody (HAMA) is slightly limited.²² Replacing murine with homologous human sequences through genetic engineering can produce “chimeric” or “humanized” antibodies.²³ Phage display is an important method for obtaining fully human antibodies against a given antigen.²⁴ In this study, we explored human single-chain variable fragments (scFvs) to extend NMOSD complement therapy. Using phage display techniques, we developed a fully human C5-targeted scFv (C5-scFv) as a therapy for NMOSD.²⁵

Methods

Standard protocol approval, registration, and patient consent

The Committee on the Ethics of Animal Experiments of Shaanxi Normal University approved all the animal experiments. Moreover, all the animal experiments followed the NIH Guide for the Care and Use of Laboratory Animals. The Ethics Committees of Tianjin Medical University approved

the collection of serum from the participants. We obtained informed consent from all the participants.

Phage display procedure and C5-scFv expression and purification

We performed the phage display selection process as previously described with some adjustments.²⁶ The semisynthetic scFv phage library (Creative Biolabs, Shirley, NY) for *Escherichia coli* TG1 bacteria was cultured and infected with M13KO7 helper phage (NEB, Ipswich, MA). We concentrated the phage library with 20% polyethylene glycol precipitation. After preparing the scFv phage library, we performed 5 rounds of panning (adsorption-elution-amplification).²⁵ After 5 rounds of selection, we isolated individual clones and identified phage clones specifically binding to antigen with ELISA.²⁵ C5-scFv expression and purification were based on a previous study with some adjustments.²⁷ To obtain a 40-mg/mL C5-scFv concentration, we concentrated the C5-scFv using Amicon Ultra centrifugal filter units (Millipore, Billerica, MA).

Surface plasmon resonance

We performed surface plasmon resonance (SPR) measurements on a Biacore T200 instrument (GE Healthcare, Chicago, IL). We used 10 mM NaAC (pH 5.5) to dilute C5. Following this, we immobilized C5 onto the surface of a carboxymethyl dextran matrix 5 sensor chip. We measured binding with a 4-(2-hydroxyethyl)-1-piperazineethanesulfonic acid buffer (pH 7.4) at 25°C as the running buffer (20 μ L/min). We injected the C5-scFv for 90 seconds over the sensor chip, followed by a 180-second washout period with the same flow rate. For each injection, we regenerated the flow cells for 30 seconds using an injection of 10 mM glycine-hydrochloric acid (pH 1.5). We calculated the antibody-antigen binding constants using Biacore evaluation software (GE Healthcare).

ELISA

We coated C5 on a 96-well streptavidin-coated plate overnight at 4°C, blocked it with 2% bovine serum albumin (BSA), and incubated it with phage supernatant as the primary antibody. We detected bound phages by adding rabbit horseradish peroxidase/anti-M13 conjugate antibody (1:1,000; Creative Diagnostics, New York City, NY) for 40 minutes at room temperature with continuous gentle shaking. We stained the wells with 100 μ L of 3,3',5,5'-Tetramethylbenzidine (MYbiotech, Xi'an, China) and stopped the peroxidase reaction with 50 μ L of 2.5 M H₂SO₄. We used a microplate reader (Bio-Rad Laboratories, Hemel Hempstead, UK) to measure the absorbance at 450 nm.

NMOSD antibodies

We obtained AQP4-IgG serum (serum_{NMOSD}) from 5 AQP4-IgG-positive patients with high AQP4-IgG titers. Shi et al.²⁸ have previously described these patients' detailed clinical information. We purified the total IgG with protein-A resin (GeneScript, Piscataway, NJ) according to a previously described protocol.²⁹ After undergoing concentration using Amicon Ultra centrifugal filter units (Millipore), the final concentration of IgG (IgG_{NMOSD}) was 15 mg/mL. We collected control serum (serum_{Ctrl}) from healthy volunteers.

NMOSD animal model induction

We purchased 8- to 12-week-old weight-matched female C57BL/6 mice from the Experimental Animal Laboratories of the Academy of Military Medical Sciences. We normally fed and maintained the mice in a suitable air-filtered environment under a 12-hour light-dark cycle. We randomly assigned the mice to different groups as follows: (1) 6 μ L of IgG_{NMOSD} and 4 μ L of human complement (hC) as the control group (n = 5); (2) 6 μ L of IgG_{NMOSD}, 4 μ L of hC, and 5 μ L of C5B3 (n = 5); and (3) 4 μ L of hC and 5 μ L of C5B3 (n = 5). We intraperitoneally anesthetized the mice with 10% chloral hydrate (3 mL/kg) and mounted a stereotactic frame (RWD Life Science, Shenzhen, China). We made a midline scalp incision to expose the bregma and lambda. For intraparenchymal injections at a skull position 2.5 mm to the right of the bregma, we made a 0.7-mm diameter burr hole with a high-speed drill (RWD Life science). We inserted a 33-G needle attached to a 25- μ L gas-tight glass syringe (Hamilton, Reno, NV) 3 mm deep to infuse 6 μ L of IgG_{NMOSD} and 4 μ L of hC with or without 5 μ L of C5B3 (total volume, 15 μ L at 1 μ L/min). We injected another group of mice with 4 μ L of hC and 5 μ L of C5B3 (total volume, 15 μ L). We maintained rectal temperature at 37°C during anesthesia. After disinfecting the scalp surface, we sutured the scalp. Seven days later and immediately before euthanasia, we anaesthetized (10% chloral hydrate) the mice and perfused them through the left cardiac ventricle with phosphate-buffered saline (PBS), followed by 4% paraformaldehyde (PFA). Following this, we processed them for frozen sectioning.

Complement-dependent cytotoxicity

We stably transfected Chinese hamster ovary (CHO) cells with human M23-AQP4 as previously described.³⁰ We cultured M23-AQP4-overexpressing CHO cells in 1640 Nutrient Mix Medium supplemented with 10% fetal bovine serum, 100 μ g/mL streptomycin, and 100 U/mL penicillin (Gibco, Grand Island, NY). In a humidified atmosphere of 5% CO₂ at 37°C, we cultured the cells. When the cells were confluent, we washed them with PBS. Following this, we added 2.5% hC to the wells with 10% serum_{NMOSD} with or without 500 μ g/ml C5-scFv (C5B3, C5B35, and C5A6) for 30 minutes. We incubated some wells with serum_{Ctrl} or different dilutions of serum_{NMOSD} with 2.5% hC and other wells with different dilutions of hC with 10% serum_{NMOSD} with or without different dilutions of C5B3. We assayed cytotoxicity using a LIVE/DEAD Viability/Cytotoxicity Kit (Invitrogen, Carlsbad, CA).

Immunocytochemistry

We incubated M23-AQP4-overexpressing CHO cells with 10% serum_{NMOSD} and 2.5% hC with or without C5B3. We washed the wells with PBS, fixed them with 4% PFA, and blocked them with 5% BSA. We incubated the cells with rabbit polyclonal anti-C5b-9 (1:100; Abcam, Cambridge, UK) primary antibodies in 5% BSA at 4°C overnight, followed by incubation with goat anti-rabbit IgG-conjugated Alexa Fluor 594 (1:1,000; Invitrogen, Carlsbad, CA) in 5% BSA. After secondary antibody incubation, we washed the cells again with PBS and examined them using a fluorescence microscope (Leica DM6000B; Leica, Wetzlar, Germany). The investigators were blinded to the experimental groups during pathology staining and analysis.

Immunohistochemistry

We selected the frozen sections (thickness, 6 μ m) through the needle tract. We permeabilized the frozen sections with cold acetone, blocked them (5% BSA), and immunostained them with the following primary antibodies at 4°C overnight: rabbit polyclonal anti-AQP4 (1:100; Santa Cruz Biotechnology, Dallas, TX), goat polyclonal anti-glia fibrillary acidic protein (GFAP) (1:1,000; Abcam), rat anti-myelin basic protein (MBP, 1:200; Millipore), rat anti-CD45 (1:100; BD Biosciences, San Jose, CA), rabbit polyclonal anti-ionized calcium-binding adaptor molecule 1 (IBA1, 1:1,000; Wako, Osaka, Japan), and rabbit polyclonal anti-C5b-9 (1:100; Abcam). Following this, we immunostained the frozen sections with the appropriate Alexa Fluor-conjugated secondary antibody (1:1,000; Invitrogen). We examined the tissue sections with a Leica DM 6000B microscope and defined the areas using ImageJ software (ImageJ 1.51j8; NIH).²⁹ The investigators were blinded to the experimental groups during pathology staining and analysis.

Statistical analyses

We present the data as mean \pm standard error of the mean. We used a 2-tailed unpaired *t* test to compare 2 groups, and we used a 1-way analysis of variance for comparisons between 3 groups. We considered a *p* value <0.05 to be significant. For our analysis, we used SPSS for Windows software (version 17.0; SPSS, Inc, Chicago, IL).

Data availability

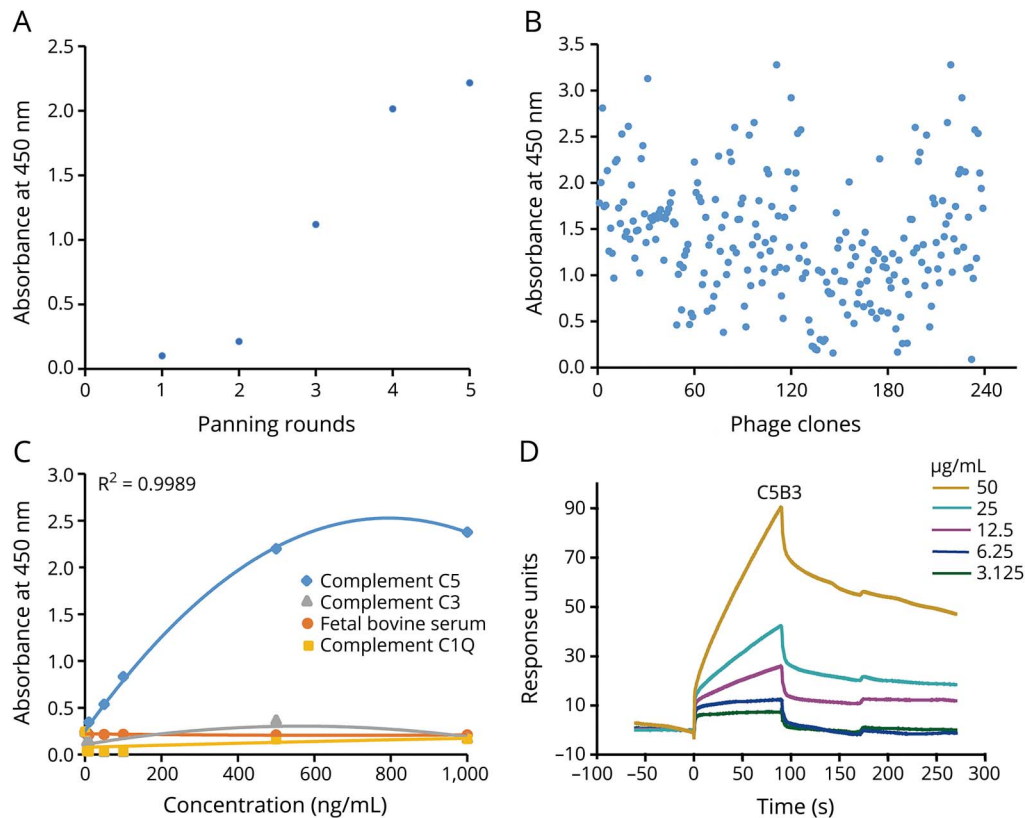
We will share the study data upon request from any qualified investigator.

Results

Phage display screened human scFv clones against C5

We performed 5 rounds of panning (adsorption-elution-amplification) of the semisynthetic scFv phage library. As shown by ELISA, the ability of the phage library to bind to C5 gradually increased (figure 1A). Following this, we tested 239 randomly chosen individual colonies from the fifth round of selection for reactivity with C5 by ELISA (figure 1B). We sequenced 32 scFvs with high-level binding activities and

Figure 1 Phage display selected human scFvs against complement C5



We coated complement C5 on a 96-well streptavidin-coated plate overnight at 4°C, blocked (2% BSA) the wells, and incubated them with phage. Following this, we performed 5 rounds of panning (adsorption-elution-amplification) and identified the phage clones specifically binding to C5 by ELISA. (A) After 5 rounds of panning, the ability of phage antibodies binding to complement C5 gradually increased. (B) As shown by ELISA, 239 randomly selected clones from the fifth round of selection reacted with complement C5. (C) C5B3 binds specifically to complement C5, but had a low affinity for control proteins (i.e., BSA and complements C3 and C1Q). (D) The SPR sensorgram shows concentration-dependent binding of C5B3 to C5. We immobilized complement C5 onto a CM5 sensor chip. We injected C5B3 for 90 seconds over the sensor chip, followed by a 180-second washout period (20 µL/min). BSA = bovine serum albumin; scFvs = single-chain variable fragments; SPR = surface plasmon resonance.

a low binding background. The analysis of the sequences led to the identification of 8 unique sequences (C5B3, C5B35, C5B98, C5B106, C5A6, C5A102, C5A121, and C5A152). Of the 32 scFvs, 9 scFvs had the same complementarity determining region (i.e., C5B3). C5B35 and C5A6 were represented 5 and 8 times, respectively (table). We evaluated C5B3 antibody specificity with different concentrations of C5 and control proteins. Our results showed that C5B3 did not bind to the control protein and had good specificity (figure 1C). In figure 1D, the SPR sensorgram shows the concentration-

dependent binding of C5B3 to C5. The affinity of C5B3 binding to C5 (K_D) was 4.395 µM.

C5B3-scFv inhibited AQP4-IgG-mediated CDC in vitro

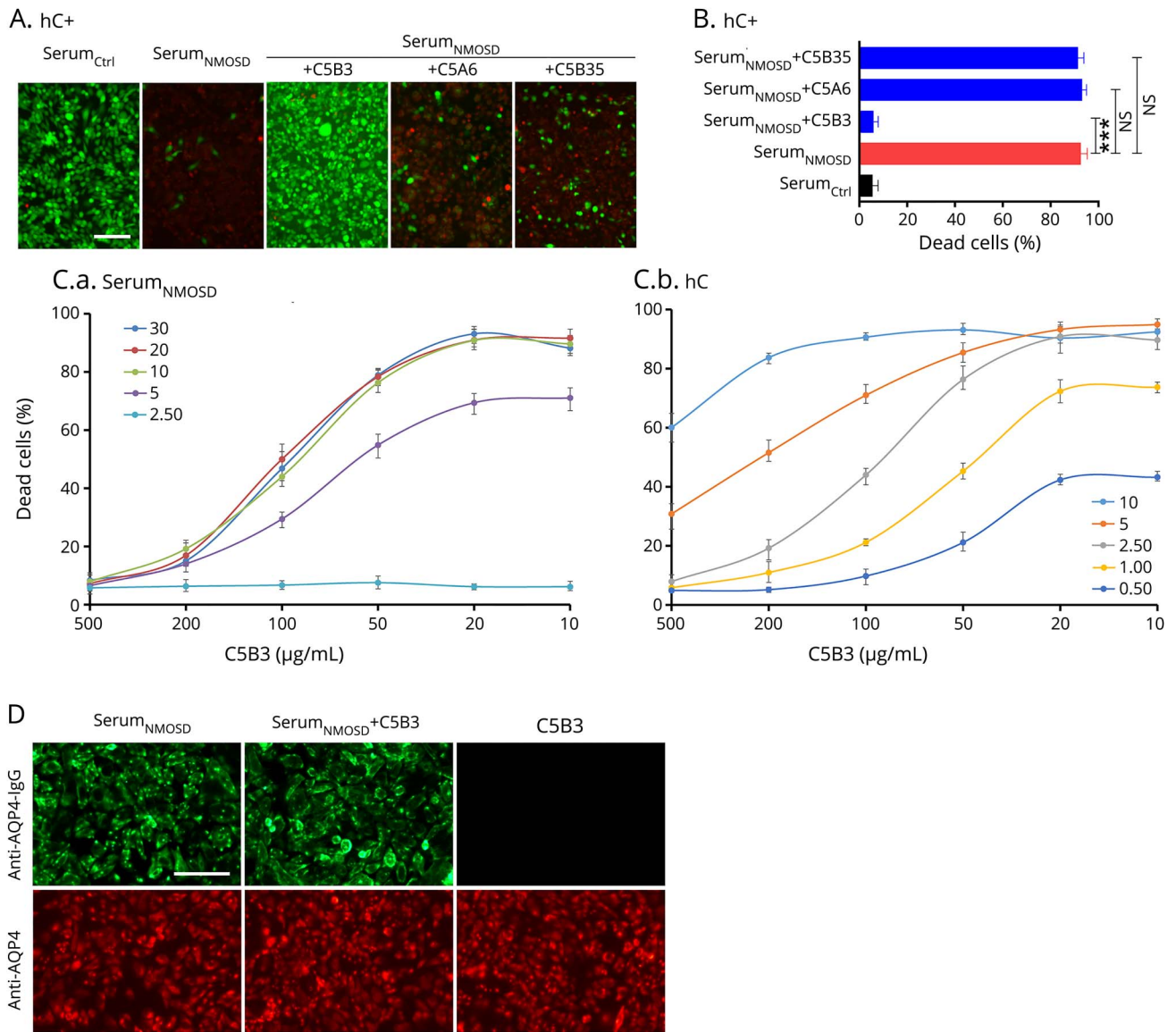
We cultured M23-AQP4-overexpressing CHO cells to confluence and incubated them with different dilutions of serum_{NMOSD} or serum_{Ctrl} with different dilutions of hC for 30 minutes. We treated some wells with different dilutions of C5-scFv (C5B3, C5B35, and C5A6). As shown in figure 2, we

Table Amino acid sequence and repeated sequences number

C5-scFv	HV-CDR3	LV-CDR3	Repeated sequences number
C5B3	AKTTRFFDY	QQARTSPST	9
C5B35	AKNRRMFDY	QQNAYFPTT	5
C5A6	AKVSTPFDY	QQPHYRPQT	8

Abbreviations: C5-scFv = human C5-targeted single-chain variable fragment; CDR = complementarity determining region; HV = heavy chain variable region; LV = light chain variable region.

Figure 2 C5B3 prevented AQP4-IgG-mediated CDC without affecting AQP4-IgG binding to AQP4



(A) After incubation with 10% serum_{NMOSD} and 2.5% hC with or without C5B3, C5A6, and C5B35, we measured CHO cells cytotoxicity with LIVE/DEAD staining. (B) The percentage of dead cells from the experiments shown in Fig A. (C.a) CDC in M23-AQP4-overexpressing CHO cells incubated with 2.5% hC and different concentrations of serum_{NMOSD} and C5B3. (C.b) CDC in M23-AQP4-overexpressing CHO cells incubated with 10% serum_{NMOSD} and different concentrations of hC and C5B3. (D) We fixed the CHO cells and incubated them with 10% serum_{NMOSD} with and without 800 µg/mL of C5B3 for immunostaining of AQP4 (red) and human IgG (green). The scale bar size for both A and D stains are all 200 µm. ****p* < 0.001. AQP4 = aquaporin-4; CDC = complement-dependent cytotoxicity; hC = human complement; IgG = immunoglobulin G.

added 2.5% hC to the wells with 10% serum_{NMOSD} with or without 500 µg/mL of C5-scFv. Figure 2A displays representative LIVE/DEAD staining, and figure 2B summarizes the statistical results. Compared with serum_{Ctrl}, serum_{NMOSD} caused marked cytotoxicity, which was rescued by C5B3 (*p* < 0.01), but not C5B35 or C5A6. This finding indicates that C5B3, but not C5B35 or C5A6, inhibits cytotoxicity; however, all the sequences specifically bind to C5. To further clarify whether the preventive effect of C5B3 is dependent on complement or AQP4-IgG, we fixed the hC at a concentration of 2.5% and displayed the cytotoxicity as a function of the serum_{NMOSD} concentration. The half maximal effective

concentration (EC₅₀) was approximately unchanged (figure 2C, left). When we fixed the serum_{NMOSD} at a concentration of 10%, we displayed the cytotoxicity as a function of the hC concentration. The EC₅₀ varies depending on the concentration of hC, which suggests that we needed a larger amount of C5B3 to block the larger amount of hC (figure 2C, right). In the control studies, C5B3 did not affect the binding of serum_{NMOSD} and AQP4. Immunofluorescence showed that C5B3 at a high concentration (800 µg/mL) had no effect on AQP4-IgG binding to AQP4 (figure 2D). Collectively, these results indicate that the protective role of C5B3 is dependent on hC, but not AQP4-IgG.

To confirm the protective effect of C5B3 on MAC formation, we immunostained the cells to detect C5b-9 as shown in figure 3. There was apparent C5b-9–positive particle deposition on the plasma membranes of CHO cells treated with serum_{NMOSD} and hC; however, deposition markedly decreased in cells treated with serum_{NMOSD}, hC, and C5B3 (figure 3A). Figure 3B shows the percentage of C5b-9–positive cells. We found a significant reduction in C5b-9–positive cells in the group treated with serum_{NMOSD}, hC, and C5B3 (20.23 ± 2.65 vs $80.88 \pm 3.54\%$, $p < 0.001$).

C5B3 decreased NMOSD mouse model lesions in vivo

To explore whether the inhibitory effect of C5B3 on AQP4-IgG–mediated CDC in vitro could be translated to an NMOSD mouse model in vivo, we intracerebrally injected 6 μL of IgG_{NMOSD} and 4 μL of hC with or without 5 μL of C5B3 into mouse brains as described in our previous reports.^{28,29,32} The mice were weight matched and in good health. At 7 days after surgery, 5 animals in each experimental group survived at the end of the experiments with a survival rate of 100%. The extensive loss of AQP4, GFAP, and MBP in the group treated with IgG_{NMOSD} and hC indicated that the mouse model can mimic the pathology of patients with NMOSD (figure 4A; see figure 4B for high magnification). In figure 4C, we quantified the areas of AQP4, GFAP, and myelin loss shown in figure 4A. Compared with the group treated with IgG_{NMOSD} and hC, the group treated with IgG_{NMOSD}, hC, and C5B3 showed greatly reduced loss of AQP4 (1.813 ± 0.1858 vs 2.669 ± 0.126 mm^2 , $n = 5$, $p < 0.01$), GFAP (0.9202 ± 0.1067 vs 1.461 ± 0.092 mm^2 , $n = 5$, $p < 0.05$), and MBP (1.034 ± 0.08372 vs 1.450 ± 0.04557 mm^2 , $n = 5$, $p < 0.05$; figure 4C). In the

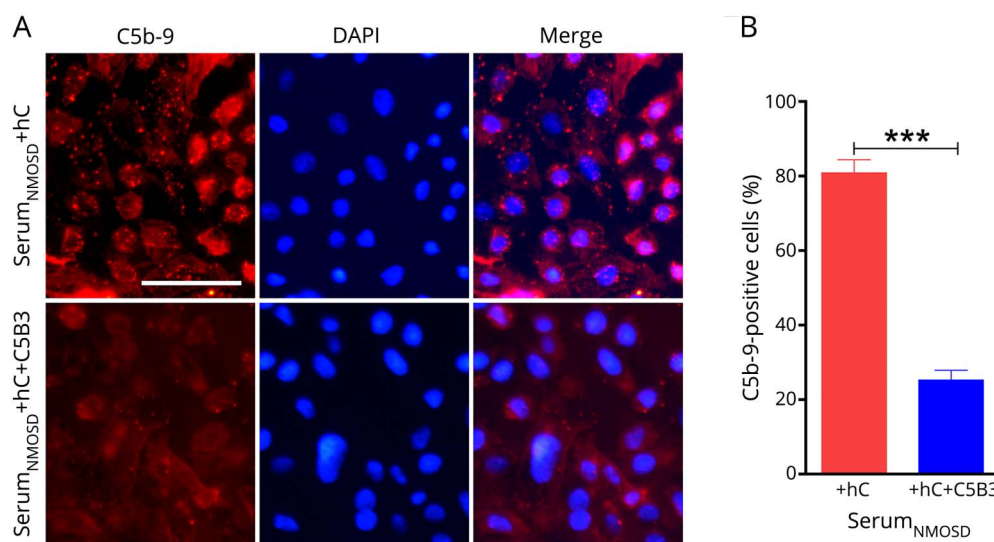
control group, we injected 4 μL of hC and 5 μL of C5B3 and found minimal loss of AQP4, GFAP, and MBP.

CNS inflammatory infiltration is an important pathologic feature of patients with NMOSD and NMOSD animal models. In the mouse brain following intracranial injections of IgG_{NMOSD} and hC, we found pronounced leukocyte infiltration, including infiltration of macrophages and active microglia. Figure 5A depicts the infiltration of CD45⁺ and IBA1⁺ cells and C5b-9 formation, and figure 5B shows the extent of infiltration. We detected a mass of CD45⁺ leukocytes, IBA1⁺ macrophages, and activated microglia in mice injected with IgG_{NMOSD} and hC. In contrast, C5B3 greatly decreased the areas of CD45⁺ leukocytes (1.449 ± 0.150 vs 2.201 ± 0.062 mm^2 , $n = 5$, $p < 0.01$), IBA1⁺ macrophages and activated microglia (1.429 ± 0.155 vs 2.068 ± 0.036 mm^2 , $n = 5$, $p < 0.01$), and the area of C5b-9 formation (0.889 ± 0.094 vs 1.433 ± 0.0545 mm^2 , $n = 5$, $p < 0.01$) in the mouse brains.

Discussion

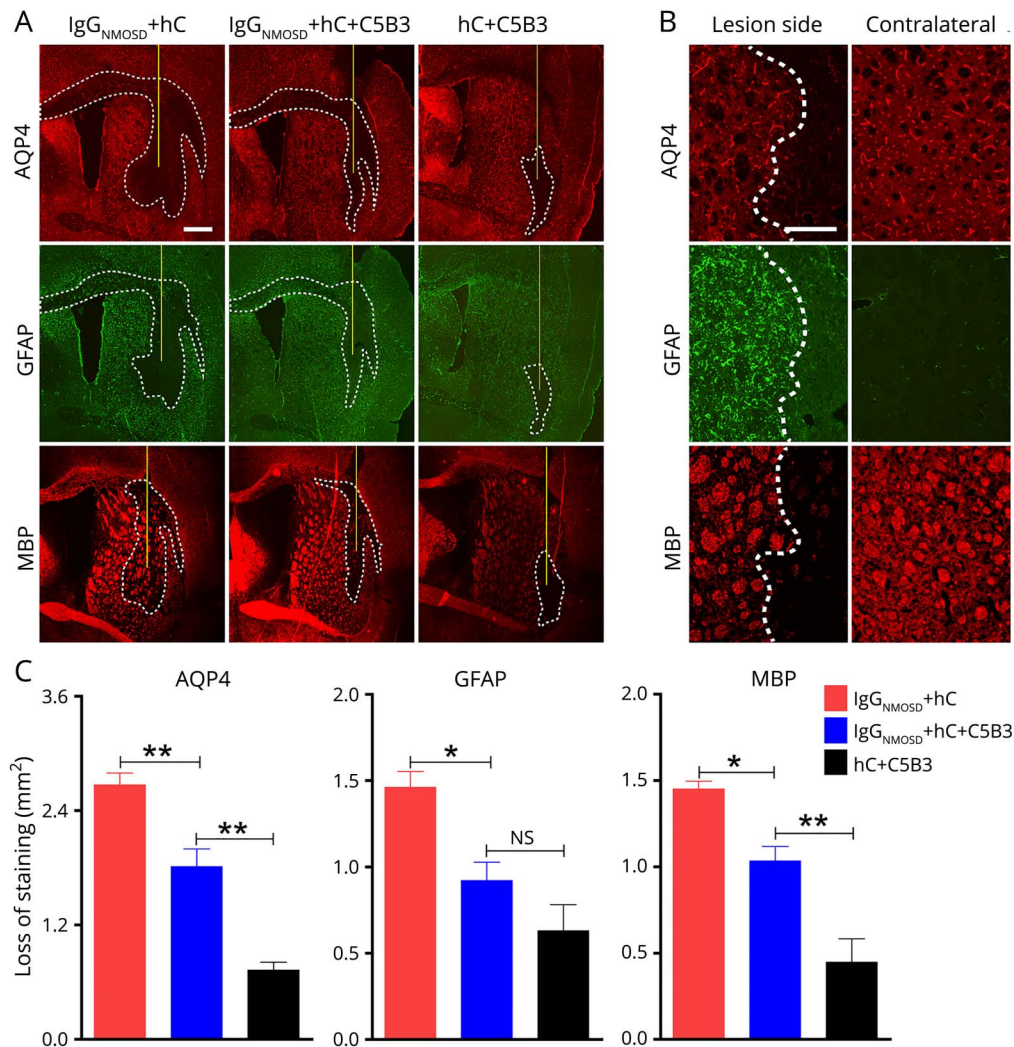
In this study, we obtained complement C5-scFvs from the human phage display library and selected the best 3 clones to test C5 specificity with ELISA. Furthermore, we investigated the efficiency of C5-scFvs in blocking AQP4-IgG– and hC–mediated CDC using M23-AQP4–transfected CHO cells and found the best sequence, C5B3. We found that C5B3 inhibited MAC formation and decreased the death rate of M23-AQP4–transfected CHO cells in vitro. We also explored the therapeutic effect of C5B3 in an NMOSD mouse model in vivo. C5B3 prevented AQP4 and astrocyte loss, decreased demyelination, and reduced inflammatory infiltration in

Figure 3 C5B3 blocked MAC formation



(A) We incubated M23-AQP4–overexpressing CHO cells with 10% serum_{NMOSD} and 2.5% hC with or without 500 $\mu\text{g}/\text{mL}$ of C5B3 for 30 minutes and fixed and stained them with anti-C5b-9 antibody. (B) We considered the red-to-blue fluorescence ratio to be statistically significant. Scale bar is 200 μm . We used a 2-tailed unpaired t test to compare the 2 groups; *** $p < 0.001$. AQP4 = aquaporin-4; hC = human complement; MAC = membrane attack complex.

Figure 4 C5B3 decreased NMOSD mouse model lesions in vivo



We injected the mouse brains with 6 μ L of IgG_{NMOSD} and 4 μ L of hC with or without 5 μ L of C5B3. (A) GFAP, AQP4, and MBP immunofluorescence at 7 days after injection. The white lines delimit the lesion with AQP4, GFAP, and MBP loss. The yellow lines represent the needle tract. Scale bar is 500 μ m. (B) High magnification of AQP4, GFAP, and MBP in injected hemispheres and noninjected contralateral hemispheres. Scale bar is 100 μ m. The white dashed lines delimit the lesion. (C) Lesion size quantification from experiments. We used 1-way analysis of variance (ANOVA) to compare between the 3 groups; n = 5/group; * p < 0.05, ** p < 0.01. AQP4 = aquaporin-4; GFAP = glial fibrillary acidic protein; MBP = myelin basic protein; NMOSD = neuromyelitis optica spectrum disorder.

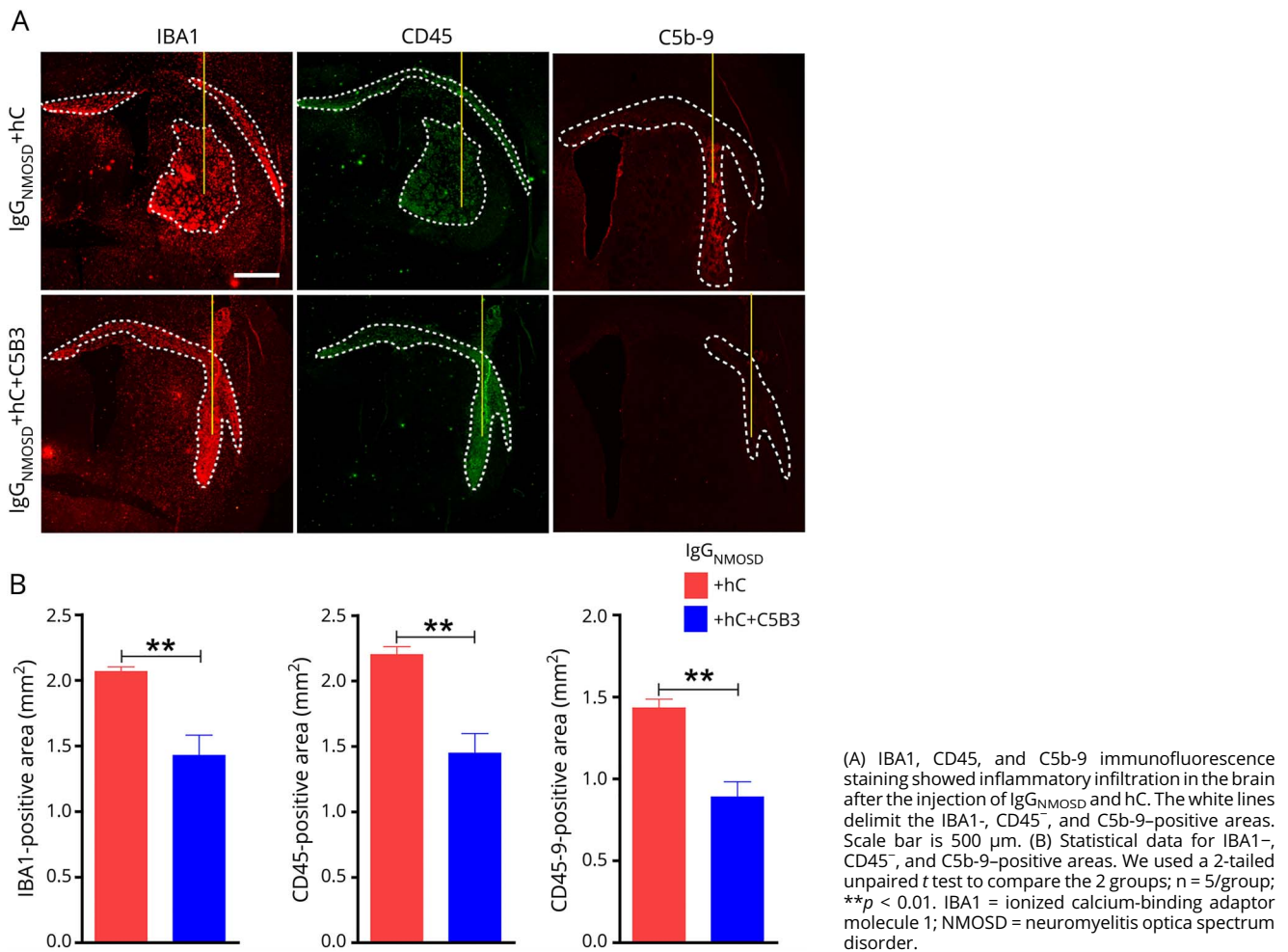
lesions. In the future, investigators should perform a comparison of the therapeutic effect of C5B3 with other monoclonal inhibitors of C5.

Monoclonal antibody therapy is a promising strategy to treat NMOSD. Several monoclonal antibody therapies are under evaluation for the treatment of NMOSD.^{18,21} Rituximab, a chimeric monoclonal antibody against CD20, has been reported to be efficacious and safe in controlling NMOSD, resulting in relapse rate reduction and disability stabilization.^{6,31} Aquaporin-4 antibody (mAb-53), a recombinant nonpathogenic human monoclonal antibody to AQP4, can bind to AQP4, but cannot activate the complement response. Although mAb-53 has not been clinically applied to patients, it has had a therapeutic effect in an NMOSD mouse model.²¹ In some case reports of patients with NMOSD, tocilizumab,

a humanized monoclonal antibody to the IL6 receptor, has significantly reduced relapse rates and possibly stabilized disability levels and is currently under development.^{32,33}

Many studies have investigated several monoclonal antibodies against complement components. Complement C1-targeted monoclonal antibodies were efficient in an NMOSD mouse model.³⁴ Eculizumab is an approved treatment for atypical hemolytic uremic syndrome and paroxysmal nocturnal hemoglobinuria.¹⁹ An open-label trial reported that eculizumab could significantly reduce relapse frequency in patients with NMOSD.³⁵ Most murine-derived monoclonal antibodies for NMOSD treatment have the potential to generate HAMA-neutralizing antibodies. The HAMA response can decrease therapeutic effectiveness and limit long-term application. In this regard, a fully human scFv would be necessary for

Figure 5 C5B3 inhibited inflammatory infiltration in an NMOSD mouse model in vivo



NMOSD treatment. Pexelizumab, which is a recombinant humanized scFv that binds to C5, was the first scFv to enter clinical trials.^{36,37} Researchers designed pexelizumab to inhibit complement-mediated tissue damage in patients after coronary artery surgery.³⁸ Compared with humanized monoclonal antibodies, C5B3 may have lower immunogenicity, which will require further research for confirmation.

The microenvironment of the lesion site after NMOSD induction is crucial for NMOSD treatment, especially concerning the control of inflammatory cells and complement reactions within the brain. In our experiment, C5B3 was effective for the treatment of AQP4-IgG-mediated lesions in an NMOSD model. C5B3 inhibited lesion formation by blocking MAC, reducing inflammation, improving the lesion site microenvironment, and reducing astrocyte damage, which protected the myelin and neurons.

There are some limitations to this study. The NMOSD model cannot fully mimic the pathogenesis of patients with NMOSD. We encourage researchers to use caution if directly extrapolating animal data to humans. Future preclinical or

clinical studies should investigate the efficacy and pharmacokinetics of C5B3 in patients with NMOSD.

Using phage display technology, we obtained a fully human scFv against C5 and provided a proof-of-concept for this scFv in NMOSD treatment. C5B3 inhibited AQP4-IgG-mediated CDC in vitro and ameliorated NMOSD mouse model lesions in vivo. Moreover, C5B3 may have low immunogenicity, which indicates that it has a high potential for future clinical translation. In the future, C5B3 may serve as a promising treatment for NMOSD.

Acknowledgment

The authors thank the patients for participating in this study and the neuroimmunology team for their experimental and technical support.

Study funding

The National Natural Science Foundation (81571596, 81771279, and 81601044) and Fundamental Research Funds for the Central Universities (GK201701009) supported this work.

Disclosure

Y.P. Yan received research support from the National Natural Science Foundation (81571596, 81771279, and 81601044) and Fundamental Research Funds for the Central Universities (GK201701009). W.L. Zhu, Z. Wang, S.Y. Hu, Y. Gong, Y.C. Liu, H.H. Song, X.L. Ding, and Y. Fu report no disclosures. Disclosures available: Neurology.org/NN.

Publication history

Received by *Neurology: Neuroimmunology & Neuroinflammation* September 17, 2018. Accepted in final form February 5, 2019.

Appendix Author contributions

Name	Location	Role	Contribution
Wenli Zhu, MD	Shaanxi Normal University	Author	Performed the experiments, analyzed the data, and drafted the manuscript
Zhen Wang, MD	Shaanxi Normal University	Author	Performed the experiments
Suying Hu, PhD	Shaanxi Normal University	Author	Performed the experiments
Ye Gong, PhD	Shaanxi Normal University	Author	Performed the experiments
Yuanchu Liu, PhD	Shaanxi Normal University	Author	Performed the experiments
Huanhuan Song, PhD	Shaanxi Normal University	Author	Analyzed the data and drafted the manuscript
Xiaoli Ding, PhD	Shaanxi Normal University	Author	Analyzed the data and drafted the manuscript
Ying Fu, MD	Shaanxi Normal University	Author	Analyzed the data and drafted the manuscript
Yaping Yan, PhD	Shaanxi Normal University	Corresponding author	Conceived and designed the study, performed the experiments, analyzed the data, and drafted the manuscript

References

- Jarius S, Paul F, Franciotta D, et al. Mechanisms of disease: aquaporin-4 antibodies in neuromyelitis optica. *Nat Clin Pract Neurol* 2008;4:202–214.
- Wingerchuk DM, Lennon VA, Lucchinetti CF, Pittock SJ, Weinshenker BG. The spectrum of neuromyelitis optica. *Lancet Neurol* 2007;6:805–815.
- Lennon VA, Kryzer TJ, Pittock SJ, Verkman AS, Hinson SR. IgG marker of optic-spinal multiple sclerosis binds to the aquaporin-4 water channel. *J Exp Med* 2005;202:473–477.
- Kleiter I, Hellwig K, Berthele A, et al. Failure of natalizumab to prevent relapses in neuromyelitis optica. *Arch Neurol* 2012;69:239–245.
- Palace J, Leite MI, Nairne A, Vincent A. Interferon Beta treatment in neuromyelitis optica: increase in relapses and aquaporin 4 antibody titers. *Arch Neurol* 2010;67:1016–1017.
- Leavitt J. Treatment of neuromyelitis optica with rituximab: retrospective analysis of 25 patients. *Yearb Neurol Neurosurg* 2009;2009:112–113.
- Miyamoto K, Kusunoki S. Intermittent plasmapheresis prevents recurrence in neuromyelitis optica. *Ther Apher Dial* 2009;13:505–508.

- Papadopoulos MC, Bennett JL, Verkman AS. Treatment of neuromyelitis optica: state-of-the-art and emerging therapies. *Nat Rev Neurol* 2014;10:493–506.
- Hengstman GJD, Wesseling P, Frenken CWGM, Jongen PJH. Neuromyelitis optica with clinical and histopathological involvement of the brain. *Mult Scler J* 2007;13:679–682.
- Hinson SR, Pittock SJ, Lucchinetti CF, et al. Pathogenic potential of IgG binding to water channel extracellular domain in neuromyelitis optica. *Neurology* 2007;69:2221–2231.
- Hinson SR, McKeon A, Fryer JP, et al. Prediction of neuromyelitis optica attack severity by quantitation of complement-mediated injury to aquaporin-4-expressing cells. *Arch Neurol* 2009;66:1164–1167.
- Roemer SF, Parisi JE, Lennon VA, et al. Pattern-specific loss of aquaporin-4 immunoreactivity distinguishes neuromyelitis optica from multiple sclerosis. *Brain* 2007;130:1194–1205.
- Ricklin D, Lambris JD. Progress and trends in complement therapeutics. *Adv Exp Med Biol* 2013;735:1–22.
- Zipfel PF, Skerka C. Complement regulators and inhibitory proteins. *Nat Rev Immunol* 2009;9:729–740.
- Ricklin D, Hajishengallis G, Yang K, Lambris JD. Complement: a key system for immune surveillance and homeostasis. *Nat Immunol* 2010;11:785–797.
- Lambris JD, editor. *Current Topics in Complement II*. New York; London: Springer; 2008.
- Jore MM, Johnson S, Sheppard D, et al. Structural basis for therapeutic inhibition of complement C5. *Nat Struct Mol Biol* 2016;23:378–386.
- Pittock SJ, Lennon VA, McKeon A, et al. Eculizumab in AQP4-IgG-positive relapsing neuromyelitis optica spectrum disorders: an open-label pilot study. *Lancet Neurol* 2013;12:554–562.
- Rother RP, Rollins SA, Mojcik CF, Brodsky RA, Bell L. Discovery and development of the complement inhibitor eculizumab for the treatment of paroxysmal nocturnal hemoglobinuria. *Nat Biotechnol* 2007;25:1256–1264.
- Araki M, Matsuoka T, Miyamoto K, et al. Efficacy of the anti-IL-6 receptor antibody tocilizumab in neuromyelitis optica: a pilot study. *Neurology* 2014;82:1302–1306.
- Tradtrantip L, Zhang H, Saadoun S, et al. Anti-aquaporin-4 monoclonal antibody blocker therapy for neuromyelitis optica. *Ann Neurol* 2012;71:314–322.
- Tjandra JJ, Ramadi L, McKenzie IF. Development of human anti-murine antibody (HAMA) response in patients. *Immunol Cel Biol* 1990;68:367–376.
- Frenzel A, Kügler J, Helmsing S, et al. Designing human antibodies by phage display. *Transfus Med Hemother* 2017;44:312–318.
- Jespersen LS, Roberts A, Mahler SM, et al. Guiding the selection of human antibodies from phage display repertoires to a single epitope of an antigen. *Nat Biotechnol* 1994;12:899–903.
- Lee CM, Iorno N, Sierro F, Christ D. Selection of human antibody fragments by phage display. *Nat Protoc* 2007;2:3001–3008.
- de Bruin R, Spelt K, Mol J, Koes R, Quattrocchio F. Selection of high-affinity phage antibodies from phage display libraries. *Nat Biotechnol* 1999;17:397–399.
- Friedman M, Nordberg E, Höiden-Guthenberg I, et al. Phage display selection of Affibody molecules with specific binding to the extracellular domain of the epidermal growth factor receptor. *Protein Eng Des Sel* 2007;20:189–199.
- Shi K, Wang Z, Liu Y, et al. CFHR1-Modified neural stem cells ameliorated brain injury in a mouse model of neuromyelitis optica spectrum disorders. *J Immunol* 2016;197:3471–3480.
- Wang Z, Guo W, Liu Y, et al. Low expression of complement inhibitory protein CD59 contributes to humoral autoimmunity against astrocytes. *Brain Behav Immun* 2017;65:173–182.
- Fang L, Wang Z, Song HH, et al. Hydroxychloroquine fails to attenuate lesion development in a mouse model of neuromyelitis optica. *CNS Neurosci Ther* 2018;24:842–845.
- Cree BA, Lamb S, Morgan K, Chen A, Waubant E, Genain C. An open label study of the effects of rituximab in neuromyelitis optica. *Neurology* 2005;64:1270–1272.
- Araki M, Aranami T, Matsuoka T, et al. Clinical improvement in a patient with neuromyelitis optica following therapy with the anti-IL-6 receptor monoclonal antibody tocilizumab. *Mod Rheumatol* 2013;23:827–831.
- Kieseier BC, Stüve O, Dehmel T, et al. Disease amelioration with tocilizumab in a treatment-resistant patient with neuromyelitis optica: implication for cellular immune responses. *JAMA Neurol* 2013;70:390–393.
- Phuan PW, Zhang H, Asavapanumas N, et al. C1q-targeted monoclonal antibody prevents complement-dependent cytotoxicity and neuropathology in vitro and mouse models of neuromyelitis optica. *Acta Neuropathol* 2013;125:829–840.
- Brachet G, Bourquard T, Gallay N, et al. Eculizumab epitope on complement C5: progress towards a better understanding of the mechanism of action. *Mol Immunol* 2016;77:126–131.
- Evans MJ, Rollins SA, Wolff DW, et al. In vitro and in vivo inhibition of complement activity by a single-chain Fv fragment recognizing human C5. *Mol Immunol* 1995;32:1183–1195.
- Thomas TC, Rollins SA, Rother RP, et al. Inhibition of complement activity by humanized anti-C5 antibody and single-chain Fv. *Mol Immunol* 1996;33:1389–1401.
- Thérout P, Armstrong PW, Mahaffey KW, et al. Prognostic significance of blood markers of inflammation in patients with ST-segment elevation myocardial infarction undergoing primary angioplasty and effects of pexelizumab, a C5 inhibitor: a substudy of the COMMA trial. *Eur Heart J* 2005;26:1964–1970.